

Dartmouth College

Dartmouth Digital Commons

Dartmouth Scholarship

Faculty Work

8-1-2016

Review of Fluorescence Guided Surgery Systems: Identification of Key Performance Capabilities Beyond Indocyanine Green Imaging

Alisha V. DSouza
Dartmouth College

Huiyun Lin
Dartmouth College

Eric R. Henderson
Dartmouth College

Kimberley S. Samkoe
Dartmouth College

Follow this and additional works at: <https://digitalcommons.dartmouth.edu/facoa>



Part of the [Engineering Commons](#), and the [Medicine and Health Sciences Commons](#)

Dartmouth Digital Commons Citation

DSouza, Alisha V.; Lin, Huiyun; Henderson, Eric R.; and Samkoe, Kimberley S., "Review of Fluorescence Guided Surgery Systems: Identification of Key Performance Capabilities Beyond Indocyanine Green Imaging" (2016). *Dartmouth Scholarship*. 3662.
<https://digitalcommons.dartmouth.edu/facoa/3662>

This Article is brought to you for free and open access by the Faculty Work at Dartmouth Digital Commons. It has been accepted for inclusion in Dartmouth Scholarship by an authorized administrator of Dartmouth Digital Commons. For more information, please contact dartmouthdigitalcommons@groups.dartmouth.edu.

Review of fluorescence guided surgery systems: identification of key performance capabilities beyond indocyanine green imaging

Alisha V. DSouza
Huiyun Lin
Eric R. Henderson
Kimberley S. Samkoe
Brian W. Pogue

Review of fluorescence guided surgery systems: identification of key performance capabilities beyond indocyanine green imaging

Alisha V. DSouza,^{a,*} Huiyun Lin,^{a,b} Eric R. Henderson,^c Kimberley S. Samkoe,^{a,d} and Brian W. Pogue^{a,d,*}

^aDartmouth College, Thayer School of Engineering, Hanover, New Hampshire 03755, United States

^bFujian Normal University, MOE Key Laboratory of OptoElectronic Science and Technology for Medicine, Fujian Provincial Key Laboratory for Photonics Technology, Fujian 350007, China

^cDartmouth-Hitchcock Medical Center, Department of Orthopaedics, Lebanon, New Hampshire 03756, United States

^dDartmouth College, Geisel School of Medicine, Department of Surgery, Hanover, New Hampshire 03755, United States

Abstract. There is growing interest in using fluorescence imaging instruments to guide surgery, and the leading options for open-field imaging are reviewed here. While the clinical fluorescence-guided surgery (FGS) field has been focused predominantly on indocyanine green (ICG) imaging, there is accelerated development of more specific molecular tracers. These agents should help advance new indications for which FGS presents a paradigm shift in how molecular information is provided for resection decisions. There has been a steady growth in commercially marketed FGS systems, each with their own differentiated performance characteristics and specifications. A set of desirable criteria is presented to guide the evaluation of instruments, including: (i) real-time overlay of white-light and fluorescence images, (ii) operation within ambient room lighting, (iii) nanomolar-level sensitivity, (iv) quantitative capabilities, (v) simultaneous multiple fluorophore imaging, and (vi) ergonomic utility for open surgery. In this review, United States Food and Drug Administration 510(k) cleared commercial systems and some leading premarket FGS research systems were evaluated to illustrate the continual increase in this performance feature base. Generally, the systems designed for ICG-only imaging have sufficient sensitivity to ICG, but a fraction of the other desired features listed above, with both lower sensitivity and dynamic range. In comparison, the emerging research systems targeted for use with molecular agents have unique capabilities that will be essential for successful clinical imaging studies with low-concentration agents or where superior rejection of ambient light is needed. There is no perfect imaging system, but the feature differences among them are important differentiators in their utility, as outlined in the data and tables here. © The Authors. Published by SPIE under a Creative Commons Attribution 3.0 Unported License. Distribution or reproduction of this work in whole or in part requires full attribution of the original publication, including its DOI. [DOI: 10.1117/JBO.21.8.080901]

Keywords: fluorescence; image guided surgery; optical imaging; fluorescence system instrumentation; intraoperative imaging.

Paper 160227VR received Apr. 11, 2016; accepted for publication Jul. 19, 2016; published online Aug. 16, 2016.

1 Introduction

In recent years, there has been an explosion of interest in fluorescence-guided surgery, which has led to a steady demand for new commercially developed and approved fluorescence imaging devices. For the greatest clinical impact, an imaging system needs to provide a solution to the immediate clinical goal with important new information that affects the patient outcome in a way that seamlessly blends into current clinical workflow. There are several new fluorescence imagers that have been cleared for the market by the 510(k) process at the United States Food and Drug Administration (FDA) for open-surgical use with indocyanine green (ICG). Beyond this, new commercial research systems with important features are regularly emerging. However, there is often a disconnect between this emergent technology and the surgeons' needs and flexibility.¹ Several reviews discuss the design, applications, and need for such imagers and tabulate the specifications of available imagers in the market.²⁻⁷ However, none of them provides direct guidance on how to choose the right imager based on objective criteria.

System selection can be subjective and dependent on the end-user's preferences; however, defining basic criteria for comparing imagers for specific applications can help the field of surgical-guidance mature in an organized manner.

The exponential growth in the field is demonstrated by the total number of published articles in the area of fluorescence-guided surgery (FGS), which has grown from under 50/year in 1995, to 100/year in 2005, and to nearly 500/year in 2015. This growth is almost equally divided between papers discussing the growing clinical imaging approaches with ICG⁸ and the growing development of targeted-molecular contrast agents for specific vascular, metabolic, or immunologic features of tissue, by the research community.^{4,9} While most ICG imaging has been performed by use of the Novadaq SPY system as it was the first to be approved in 2005, several new systems have gained 510(k) clearance in the last 2 years, as shown in Table 1. These are all approved for procedures involving imaging blood flow, tissue perfusion, and transfer circulation in free flaps, plastic surgery, and reconstructive surgery. Despite the availability of these technologies, most surgeons still rely largely on visual and tactile cues combined with presurgical radiologic imaging to guide tissue resection. The potential benefit to surgical patients for improving tissue identification based on molecular differences,

*Address all correspondence to: Alisha V. DSouza, E-mail: alisha.v.dsouza@dartmouth.edu; Brian W. Pogue, E-mail: brian.w.pogue@dartmouth.edu

Table 1 FDA clearances through the 510(k) process based on the device being safe and effective, with substantial equivalence to a predicate device. These are all ICG fluorescence imaging systems shown along with their year of premarket approval by FDA, case number, and the indications that they are approved for.

Company	Fluorescence imaging system	Year approved/ 510(k) cleared	FDA 510(k) number	Indication approved for
Novadaq Technologies, Inc.	SPY imaging system	2005	K042961	Blood flow
Novadaq Technologies, Inc.	SPY imaging system SP2000	2007	K063345	Tissue perfusion and transfer circulation in free-flaps, plastic, and reconstructive surgery
Novadaq Technologies, Inc.	SPY fluorescent imaging system SP2001	2008	K073088	510(k) with SPY SP2000
Novadaq Technologies, Inc.	SPY fluorescent imaging system SP2001	2008	K073130	510(k) for modified device
Novadaq Technologies, Inc.	SPY intraoperative imaging system	2011	K100371	Additional gastrointestinal imaging
Hamamatsu Photonics K.K.	PDE photodynamic eye	2012	K110480	510(k) with SPY K063345 and K073130
Hamamatsu Photonics K.K.	PDE Neo	2014	K133719	510(k) with PDE K110480 for modified device
Fluoptics	Fluobeam 800 clinical imaging device	2014	K132475	510(k) with PDE
Quest Medical Imaging	Artemis ^a light engine	2015	K141164	510(k) with Karl Storz and Olympus Winter
Quest Medical	Artemis ^a handheld imaging systems	2015	K143474	510(k) with PDE and Fluobeam 800
VisionSense Ltd.	VS3-IR-MMS system	2015	K150018	510(k) with SPY 063345

^aThe Artemis system is now called Quest Spectrum.

particularly to those undergoing removal of cancers, is a compelling force driving the research and development in the field of FGS. Using molecular signals in the surgical field is a natural progression that follows the development of molecular pathology to identify lesion phenotype in conjunction with image guidance from MRI or CT, as a decision tool for patient management; there is a compelling evidence that these phenotypes can be imaged *in vivo* to allow better real-time definition of the surgical margin.^{10–16}

In addition to ICG, there is extensive ongoing research using fluorescein and 5-aminolevulinic acid-induced protoporphyrin IX (PpIX) imaging for neurosurgery,^{17–21} a procedure that has gained clinical approval in a handful of countries (Approved by the European Medicines Agency in September 2007 and is approved for use in all European Union, European Economic Area, and European Free Trade Association states). Additionally, PpIX fluorescence imaging using blue light illumination has local approvals in some countries for subspecialty use in bladder cancer detection^{22–24} and gynecologic oncology^{25–27} with clinical trials underway. These fluorophores are FDA approved for certain indications and emit fluorescence within the visible light range; therefore, existing surgical microscopes can be modified with some basic filters to allow surgeons to switch back and forth between white-light and fluorescence modes. However, while there is apparently good sensitivity, the lack of high specificity of PpIX in some indications has limited the widespread adoption of this endogenous metabolic fluorophore. Moreover, the emission bands correspond to the visible light window and hence suffer from high background autofluorescence. The high absorption from biological chromophores in the visible light window also limits sensitivity to these fluorescence emissions

at depth allowing only surface imaging. Near-infrared (NIR) fluorophores, on the other hand, emit in a wavelength window with very low tissue autofluorescence, and also have greater penetration depth due to the reduced hemoglobin absorption in the 650- to 900-nm range.²⁸ Available within this range is methylene blue, a weakly fluorescent visible blue dye that is currently approved for use as a visible stain for lymph node mapping.² While some research groups have investigated its use as a far-red fluorophore,²⁹ the low fluorescence yield and lack of any functional groups for addition of ligands have limited its use in clinical applications. ICG is the only approved fluorophore in the NIR-window and several imagers have been designed and commercially launched to allow ICG guidance in surgery for blood flow assessment,^{30–32} hepatic function assessment,^{33,34} and vessel patency and perfusion evaluation especially in reconstructive^{35,36} and bypass surgeries.^{37,38} The low tissue autofluorescence in the NIR-wavelengths further simplifies the task of filtering out background signals, and since ICG is the primary reimbursable agent today, almost all imaging device companies have built systems specifically for ICG imaging. Currently, there is growing use of ICG in off-label and investigational applications such as lymphatic imaging³⁹ and surgical procedures such as sentinel lymph node identification and mapping.^{40–42} Yet a strong motivation for future development in the field is to achieve the potential for imaging molecular tracers that report on new vascular, structural, metabolic, immunologic, or genetic features of the tissue.⁴³

Surgical oncology is in a position to benefit greatly from fluorescence imaging technology, and targeted-molecular surgical guidance in particular, is poised to follow the widespread adoption of molecular pathology phenotyping.⁴ Several

companies are now producing NIR-emitting agents that can be imaged using systems designed for ICG, but with substantially higher fluorescence yields than ICG, and availability of molecules that can be conjugated to targeting moieties for future indications that have molecular specificity: IRDye 800CW (LI-COR Biosciences, Lincoln, NE), ZW800-1⁴⁴ (Curadel ResVet Imaging, Worcester, Massachusetts), and VivoTag 800 (PerkinElmer, Hopkinton, Massachusetts). As applications emerge with specific agents designed for molecular diagnostic imaging, the sensitivity and dynamic range requirements will vary greatly from the current paradigm of ICG flow imaging—typical ICG studies are performed with mg/ml level concentrations in the blood, whereas molecular probes are typically imaged at $\mu\text{g/ml}$ to ng/ml concentration levels. The sensitivity along with the interplay of various factors that affect system performance such as ambient room lighting, image threshold and visualization, ultimately decide the apparent signal-to-background ratio (SBR) performance of a system within the surgical environment. Using systems in a “real-time” mode that display the fluorescence signal in a video feed imposes restrictions on the system sensitivity. This is particularly true in open surgery in which the operation is conducted under bright lighting; this is less of a challenge in minimally invasive surgery in which the procedure can take place in a darkened room. The lack of professional society guidance or standard documents on system quality and accuracy assessment further complicates matters, as there is no single test to compare systems under standard conditions as yet, and hence any SBR performance limitations are established based on clinical trials. Several research groups have been discussing the challenges in defining standardized testing platforms and have been working toward designing appropriate phantoms;⁴⁵ these advancements will pave the way for establishment of sensitivity limits of systems and improve our understanding of their utilities in studies involving microdoses of tracer administration.

While system sensitivity is critical for microdose-level tracer administration, this requirement is not as important in ICG imaging. Trade-offs that sacrifice SBR in favor of functional utility result in a more usable and flexible device. However, several FDA-approved commercial imagers do not yet have the ability to simultaneously capture and register white-light and fluorescence images, or operate reliably under operating room light conditions. This limitation requires the surgical team to switch between viewing the imager display and the surgical field, making fluorescence imaging cumbersome and limited in its ability to accurately register fluorescence-labeled tissues with what is seen with visible light; the surgeons now need to mentally register the while-light illuminated field in front of them, with the fluorescence intensity image devoid of major anatomical landmarks. Furthermore, providing information in a useful manner is often an understated requirement for the successful design and use of such imagers. While the current FDA-approved systems have been instrumental in launching fluorescence-guided surgery into growing clinical use, we believe that identifying the most important basic requirements from fluorescence imagers must be re-evaluated to address the unmet needs through future systems that are currently in the developmental phase. Figure 1 shows a panel of figures demonstrating the use of fluorescence imaging, and progression of fluorescence imaging devices with custom devices leading the way and FDA approved following along.

In this review paper, we describe the key engineering design criteria and the desirable features of a fluorescence

guidance system for open-surgical use; this discussion of desirable features is supplemented with a description of system instrumentation in the sections that will follow. The current available commercial imagers are compared in tables on the basis of functionality, usability, and technical specifications. Fluorescence microscopy systems, including surgical microscopes and confocal microscopes, were outside the scope of this review of open wide-field imagers and have not been discussed herein because the technological goals and functionality of these are quite different from open-surgical systems.

2 System Uses and Feature Goals

The overall goal of every fluorescence imager is to provide information on the distribution of the weak (relative to white-light reflectance) fluorescence signal within the surgical field. Clinical compatibility is improved by providing the information in a user-friendly, distraction-free manner, while minimizing background signals and noise. This can be simplified to the singular goal of maximizing the SBR to distinguish between diseased versus disease-free tissue or to identify tissue to save, such as nerves and blood vessels, among tissue being resected. However, SBR on its own does not make a system description complete and does not mean much without the right means to convey this information to the user. Achieving high SBR in a surgical environment is a complicated problem influenced largely by the level of ambient lights. Surgeons rely on visual information to identify landmarks and are trained to identify tissues in their native pink-red hues; any additional fluorescence information, especially that from outside the visible range of the light spectrum, must therefore be coregistered to the white-light field. These issues lead to the need to be able to view both white-light RGB and fluorescence images in real time on a display. Furthermore, operation rooms are well-lit spaces, and imagers that operate only in low light will have limited adoption in most clinical procedures.

As the field of fluorescence imaging for guidance during open surgery moves toward adoption of targeted-fluorescent probes and the quantification of disease biomarkers,⁹ the technical performance demands of fluorescence imagers will increase. While reliable absolute quantification in an open setup has not yet been fully realized and is challenging to achieve, there have been significant advances in ratiometric methods, in which tracer combinations were used to quantify receptor and molecular concentrations.^{48,49} There has also been recent growth in the development of diagnostic agents that would be administered at microdoses as compared to therapeutic agents, to match the receptor concentrations available in tissue. This latter issue would demand high sensitivity of fluorescence detection of probes present in the nanomolar concentration range. Based on these needs, a listing of key desirable features of an open fluorescence imager is as follows:

- i. *Real-time overlay* of white-light reflectance and fluorescence images;
- ii. Fluorescence-mode operation with *ambient room lighting present*;
- iii. *High sensitivity* to tracer of interest;
- iv. Ability to *quantify* fluorophores *in situ*;
- v. Ability to image *multiple fluorophores simultaneously*; and
- vi. Maximized *ergonomic use*.

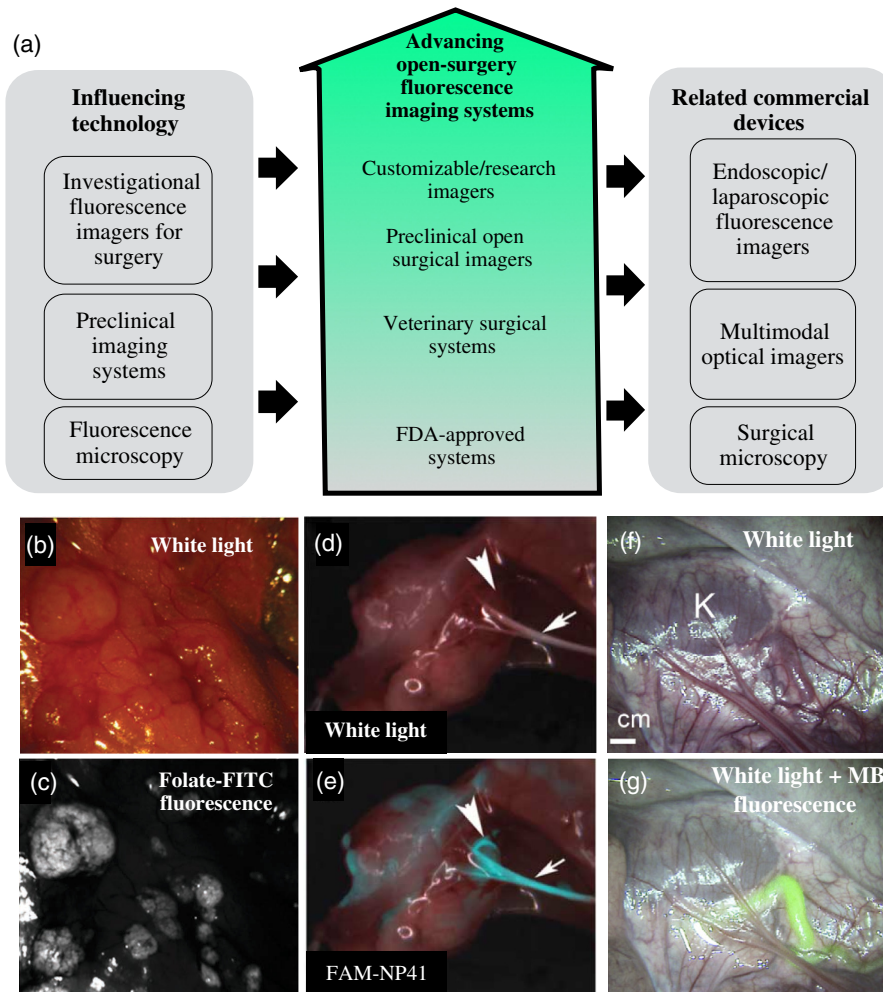


Fig. 1 (a) Demonstrates the progression of systems in terms of their regulatory approval status along with parallel technologies. On the left, research-grade surgical fluorescence imagers, preclinical devices, and microscopy devices have served as contributors to the development of open-surgery fluorescence devices. On the right, the related commercial technologies, such as endoscopic imagers, multimodal imagers, and surgical microscopes, are specialized technologies that have greatly benefited from advancement in open-surgery fluorescence imagers. The central arrow illustrates the technological progression of imagers with FDA-approved systems at the trailing end, and customizable devices leading the technology development. (b)–(g) Show examples of surgical fields paired with white-light reflectance (up) and fluorescence images (bottom) shown for various applications.^{10,46,47} Panels (b) and (c) show white-light and fluorescence images, respectively, from the first in-human example of *in situ* ovarian cancer delineation using folate receptor- α targeted-fluorescent agent (reprinted by permission from Macmillan Publishers Ltd., Nature Medicine,¹⁰ copyright 2011). Panels (d) and (e) show white-light reflectance and white-light reflectance with pseudocolor fluorescence overlay, with Fluorescein-NP41 highlighting the peripheral nerves (reprinted by permission from Macmillan Publishers Ltd., Nature Biotechnology,⁴⁶ copyright 2011). Panels (f) and (g) show ureters highlighted by methylene blue fluorescence, reprinted from Matsui et al.,⁴⁷ with permission from Elsevier.

To fully appreciate the complexity of enabling all these features, a discussion of current instrumentation is necessary; this is provided in Sec. 3. We then discuss each of the above listed features in detail in Sec. 4.

3 Imaging System Components and Instrumentation

The basic components of a fluorescence imager are (i) spectrally resolved light source(s), (ii) light-collection optics and filters, (iii) camera(s), (iv) instrument control, acquisition, and display software, and (v) computing, input, and display hardware.

3.1 Excitation Light Source

Choice of excitation light source is based on the spectral bandwidth, solid angle of output beam, output efficiency, and regulatory considerations. Commonly used excitation sources are (i) filtered broadband lamps, (ii) laser diodes, and (iii) light-emitting diodes (LEDs). Ease of filtering at detection, illumination of large field of view (FOV), output fluence rate, mounting requirement, and cost are the main factors that influence the choice of excitation source type. Among available options, filtered lamps have the lowest efficiency, largest spectral bandwidth, and largest solid angle, and hence least spatial and spectral confinement. Furthermore, a large fraction of the

output photons is rejected at the excitation filter resulting in high heat dissipation, thus making their use cumbersome and suboptimal. Such excitation source setups are seen currently in surgical microscopes.

Laser diodes have the highest spatial and spectral confinement of all sources. The low spectral bandwidth allows maximum excitation light filtering at the fluorescence detection camera. High-power options are available to deliver the best light fluence rate for low fluorophore concentrations, but safety concerns related to maximum permissible exposure limits for skin and eyes complicate the regulatory approval of systems that use these. Moreover, beam expanders would be necessary to ensure illumination of large FOVs. Laser diodes also require precise temperature and current control to ensure fidelity of the output spectrum and power, thus necessitating additional hardware, and remote mounting away from the patient. Such systems would use fiber coupling from the light source to the illumination head. These are seen in the Fluobeam and Curadel Lab-Flare systems.

LEDs provide a trade-off among output power, efficiency, cost, and spectral bandwidth. With the growth of the LED market, it is becoming increasingly economical to produce high-power LEDs. To ensure homogeneity of the excitation field, LEDs would need to be combined into an array. However, one of the major drawbacks of using LEDs is that when fluorophores with small Stokes shifts are used, there will be leakage of excitation light past the emission filter leading to reduced SBR. An excitation filter would thus need to be used to confine the output of the light source. Some of the newer imagers such as PerkinElmer Solaris and SurgVision Explorer Air system utilize LED-based excitation, and we should expect to see further increase in their use.

3.2 Collection Optical Components and Emission Filters

Multiple trade-offs exist when discussing collection optics. These are FOV size, depth of field, lens F -number, and operating distance. Collection optics may be designed for fixed magnification or variable magnification depending on the need to have variable field size and operating distance. Most common imagers have a working distance of 10 to 30 cm with a maximum FOV size of about $15 \times 15 \text{ cm}^2$, but the tolerance for focus errors varies among manufacturers and end users.

Emission filter design and choice are critical in maximizing detection sensitivity by limiting background light. Filter choice is influenced by spectral overlap among the reflected excitation light, ambient lighting, and the Stokes shift of fluorophore of interest. Fluorophores with large Stokes shift such as PpIX, which can be excited in the blue range ($\sim 405 \text{ nm}$) and detected in the red range ($\sim 635 \text{ nm}$), pose few problems, whereas those that have significant overlap between absorption and emission spectrum such as ICG, require more careful selection (See Fig. 3). Longpass, bandpass, and notch filters are broadly the categories for selection. Interference filters generally provide superior out-of-band rejection and transmission in the passband as compared to absorption-based filters. Spectral characteristics of filters also vary with incidence angle of light and there will be transmission of undesirable excitation light at high incidence angles. This along with the excitation leakage through the rejection band determines the noise floor of a device and hence affects its sensitivity.

3.3 Imaging Sensor

The factors that influence detection performance of the camera are dynamic range, read-out rates, pixel resolution, and on-chip gain. For quantitative imaging, bit depths of 10-bit or more are desirable to provide signal detection of 2 to 3 orders of magnitude while maintaining a low noise floor. Charge-coupled device (CCD)-based cameras are used in fluorescence imagers almost ubiquitously, but suffer from low quantum efficiency in the far-red and NIR-wavelength range and slow read-out time ($<30 \text{ Hz}$). They can achieve low read-out noise when cooled, generally have high resolutions, and can be used with 16-bit A/D converters. Further improvements in sensitivity are achievable with electron multiplied-CCDs (EMCCD) and intensified-CCDs (ICCD); these can provide analog gains of over $1000\times$ and are of benefit when signal intensity is very low, but signal quality can degrade at high noise levels; these trade-offs would need to be considered carefully. The available quantum yield of sensors in the far-red- and NIR-wavelength regime can drop off significantly from the visible region, and this too will affect appropriate camera/sensor selection on a system. Almost all commercial fluorescence imagers use CCD cameras and the SurgVision system uses an EMCCD camera. The scientific-CMOS (sCMOS) cameras are now a contender against CCD cameras as they provide high read-out rates, high bit depth, and the specific advantage of many more pixels per frame. In addition to the high read-out rate and high bit depth, the compact size, light weight, and low read-out noise make sCMOS cameras the sensor of next-generation fluorescence imagers. One of the drawbacks, however, is the higher cost as compared to standard CMOS technology. Among the commercial systems available, the PerkinElmer Solaris is the only system that uses an sCMOS camera. More sophisticated camera configurations such as multispectral cameras, though rarely used in most systems, will be discussed briefly in Sec. 4.1.

3.4 Software Control, Computing, Data Storage, and Display Hardware

Software designs vary in the degree of user customizability; those that target clinical use generally have the least flexibility while investigational systems and research-oriented systems allow a good deal of user customization. With growing bit depths, high-speed data transfer and data storage become important considerations. Imaging and storing large video sequences, potentially from multiple cameras, can result in several gigabytes of imaging data per hour—storing one hour of single channel $1024 \times 1024 \text{ pixel}^2$ 8-bit fluorescence data at 30 fps for an hour would need $>100 \text{ GB}$ of space—posing a significant data management challenge. One approach to tackle this is to store compressed video files only and save data into an 8-bit format, even if the camera provides >10 -bits per pixel. Alternative strategies include saving user-prompted snapshots from a continuous video stream. The ability to customize storage and export on to external drives or servers may be a solution as well, but local protected storage is likely the best candidate for clinical systems to maintain Health Insurance Portability and Accountability Act compliance. However, data storage may be critical in research settings, to allow postprocessing, and image analysis postacquisition. Systems such as the PDE Neo lack on-board storage options and provide only screen captures, which is non-ideal and nonquantitative.

As devices grow in sophistication, software control of instruments becomes more complex especially when multicamera systems are used. On-board GPUs are often necessary for simultaneous overlay and streaming. It is important that systems be customizable yet easy to use for clinical staff and surgeons. The software functionality also directly ties-in with data visualization and display optimization. Need for ROI intensity measurement tools, and on-screen window-level and compression options⁵⁰ will increase as systems are used for quantitative or semiquantitative imaging, and as image bit depths exceed the display bit depths. Software design is the most understated aspect of fluorescence imagers, but since their use during surgery would need seamless integration with the surgical protocol, robust, intuitive design is key.

4 Design Goals and Analysis of Key Features

4.1 Real-Time Overlay of White-Light Reflectance and Fluorescence Images

Most FDA-approved imagers, such as Novadaq SPY, Hamamatsu PDE Neo, and Fluoptics Fluobeam 800, are single channel fluorescence video/image display systems. However,

imagers that have the ability to provide the fluorescence image overlaid on a white-light illuminated RGB image in a real-time video stream would provide richer and more complete information to a surgeon/user. To produce such images in real time is significantly more complex than a single channel fluorescence video stream. While there are several approaches for achieving overlaid data, wavelength-based separation of fluorescence (>650 nm) and visible white light (<650 nm) is the main principle upon which imager designs are based.

The most commonly employed technological approaches for achieving simultaneous white-light and fluorescence imaging are use of beam splitters and multiple cameras or multispectral cameras that separate visible and far-red and/or NIR-wavelengths within the camera itself using prisms and multiple CCD or CMOS sensors. The Flare intraoperative prototypes from the Frangioni laboratory use three cameras,⁴¹ and Curadel's Lab-Flare imager, based on the Flare prototype, uses three CCD sensors within a single camera body to simultaneously image two fluorescence channels and a white-light RGB channel, by removing the ~800-nm (NIR) fluorescence component, the ~700-nm far-red fluorescence component, and using the remainder to produce the RGB image, as shown in Figs. 2(b) and 2(d). The Quest Spectrum system (previously called

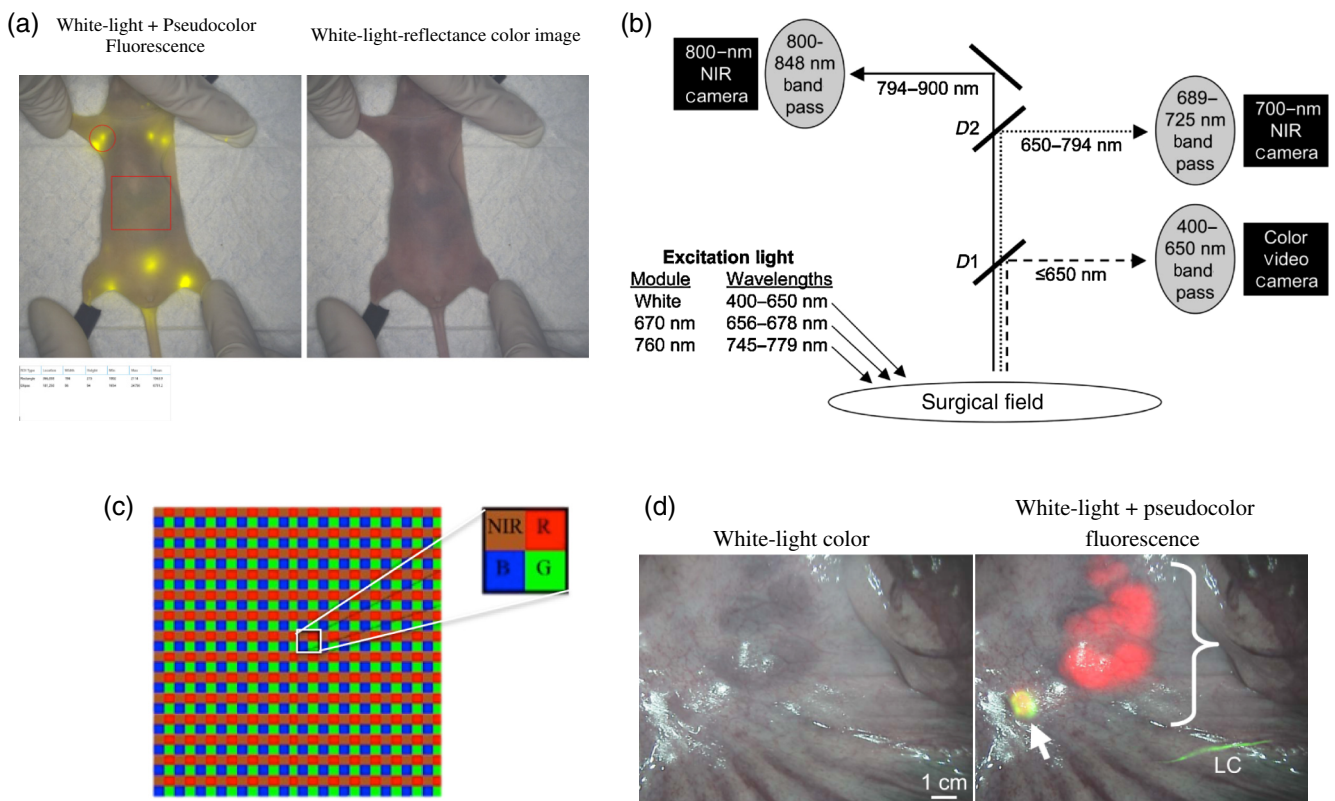


Fig. 2 Shows various white-light and fluorescence overlay schemes. (a) Shows a screenshot from the PerkinElmer Solaris imager during lymphatic imaging (image courtesy of PerkinElmer). The imaging windows display white light and the fluorescence overlaid on the white-light images simultaneously. User processing controls, such as ROI and display gain adjustments, are also available. (b) Shows the commonly used wavelength-based separation of collected light using dichroic mirrors and filters as seen in the Flare prototype system (reprinted from Troyan et al.⁴¹ with permission of Springer), Curadel Lab-Flare uses a similar setup with slightly different wavelength specifications on beam splitters and emission filters. (c) The modified Bayer filter is an alternative approach to perform simultaneous NIR detection, though this approach limits the active area for the fluorescence channel, reducing sensitivity.⁵¹ (d) Shows an example of simultaneous imaging and display of 700-nm (red) and 800-nm (green) fluorescence channels from the Flare prototype with the mesenteric lymph nodes highlighted by methylene blue (brackets) and a sentinel node (arrow) highlighted by ICG, reprinted from Troyan et al.⁴¹ with permission of Springer.

Artemis) achieves similar wavelength-based separation using prisms within a single camera, and can simultaneously image and overlay two NIR channels (700 to 830 nm and 830 to 1100 nm) on the white-light RGB image stream. However, expansion to more channels would require additional cameras/sensors for simultaneous acquisition. VisionSense Iridium also uses two CCD sensors to produce simultaneous white-light RGB and NIR fluorescence images from the ~800-nm emission channel and merges the two in real time. These approaches work well in practice, allow independent gain adjustments for each channel, and do not require sequential pulsing of excitation lights. The SurgVision and PerkinElmer Solaris systems, on the other hand, feature two cameras, one for white-light image acquisition and one for fluorescence acquisition, with overlay capability. A screenshot of the Solaris display in Fig. 2(a) shows “white-light RGB” and “white-light RGB + fluorescence overlay” images showing fluorophore uptake in murine lymph nodes. Additional considerations for multicamera setups include coregistration of the various video streams and magnification corrections. For example, Novadaq SPY uses two cameras that are not coregistered and have different pixel dimensions and zoom, as such no overlay functionality has been implemented, and white-light images are available only in snapshot mode.

Other related approaches employ Foveon X3 sensors (HyperEye Medical System, Mizuho Medical, Japan)⁵² to detect unabsorbed NIR light or modify the Bayer filter pattern and filter the NIRF signal at the entrance to the sensor,⁵¹ thus separation happens within the camera itself [see Fig. 2(c)]. These approaches, while overcoming the problem of merging multiple

streams, can be limited in their sensitivity to weak fluorescence emissions, which is most significant for targeted tracers at low concentrations in tissues.

The optimization of fluorescence visualization and displays is often underreported as systems are only now beginning to exploit overlay-based displays. With the growth in use of 10- to 16-bit acquisition cameras, proper scaling and mapping of displays on traditional display monitors are an additional concern. Application of appropriate transparency functions to the fluorescence overlay, choice of appropriate colormaps, and need for compression⁵⁰ techniques to display high bit depth images are important areas with only limited discussion in the literature. The field of high dynamic range (HDR) imaging has allowed optimal display of HDR data, yet this approach has not penetrated into medicine much as of today. As fluorescence imagers incorporate simultaneous multiple channel imaging, this aspect will gain greater importance. Elliott et al.⁵³ provide a set of guidelines for effective visualization of fluorescence during surgery using surgical microscopes, which are applicable to open surgery as well.

4.2 Fluorescence-Mode Operation with Ambient Room Lighting Present

For an imaging system to be easily translatable into a surgical suite or clinical environment, it is desirable that it operates under room lights and provides reasonable SBR. This issue is critical, especially when working with low fluorophore concentrations and when quantitation is necessary. Figure 3(e) shows a plot of the most common room light sources, such as tungsten bulbs,

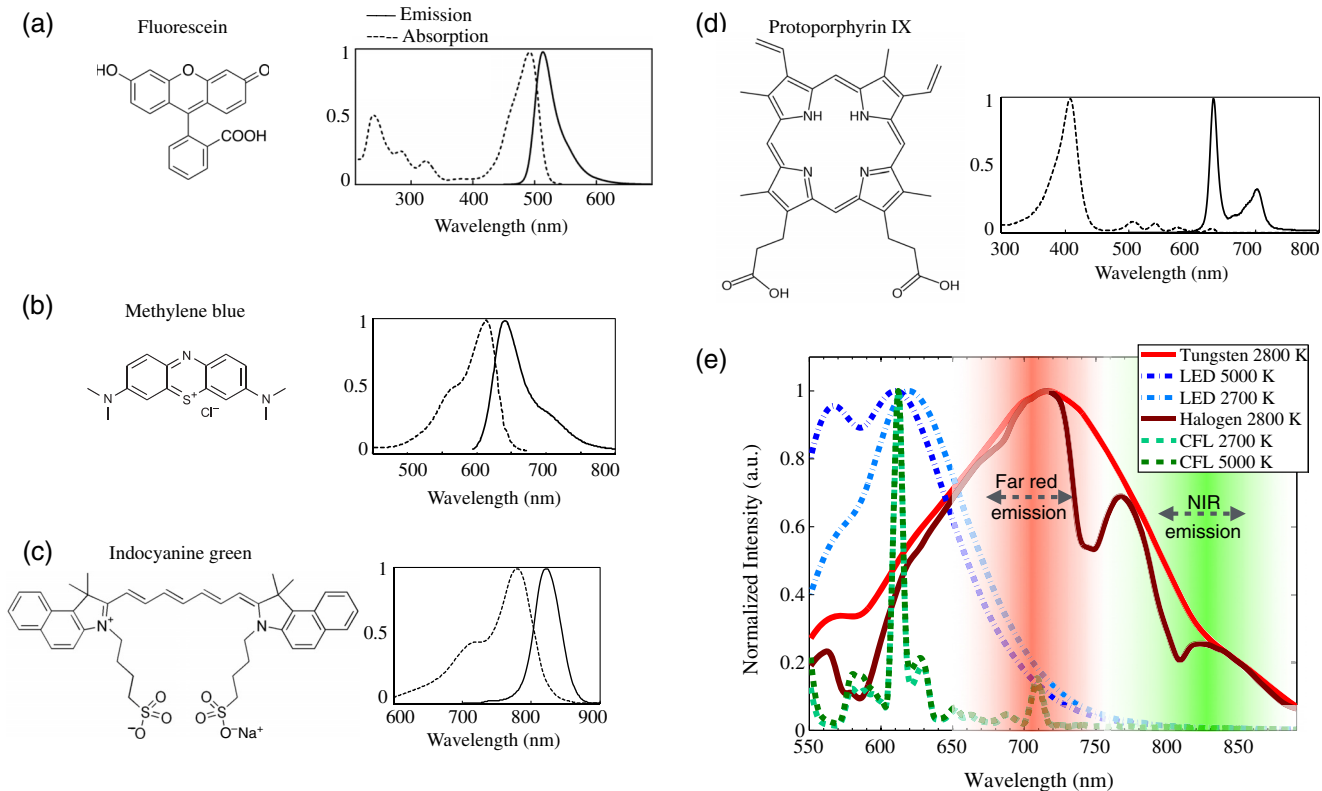


Fig. 3 (a)–(d) The chemical formulas are shown along with absorption and emission spectra of the major FDA-approved fluorescent dyes such as fluorescein, PpIX, ICG, and methylene blue. (e) The normalized emission spectra are shown for common light sources used in surgery.

halogen bulbs, compact fluorescence lights, and the newer LED lights. It can be seen that tungsten and halogen lamps have significant output in the 600- to 850-nm range and may thus contribute a major portion of the detected signal during any red to NIR fluorescence imaging. Use of these lamps in rooms is seeing a declining trend, to the ultimate benefit of fluorescence imagers. As a general guideline for researchers and other users of such systems, use of tungsten and halogen lamps, or sunlight, should be avoided completely. Both LEDs and compact fluorescent lights (CFL) have minimal signal contribution over 780 nm and thus imaging of ICG and similar NIR fluorophores in rooms lit with these sources should be attainable with simple filtering techniques. However, it should be noted that CFL lights can often emit in the 700- to 800-nm wavelength range during the warm-up phase, which can last 5 to 10 min (data not shown), and thus contamination of detected fluorescence can occur at these times. For imaging fluorophores in the visible to far-red window, i.e., 500 to 750 nm, normal room lighting would contribute to the detected signal and sophisticated background removal methods are necessary. Pulsing the LED or laser diode excitation light sources in a manner that is synchronized to a gated- or shuttered-detector system, such as CMOS or ICCD camera,⁵⁴ is one technique that may be employed to address background contamination. Similar background mitigation can be achieved using frequency modulation and lock-in detection.⁵⁵ Finally, additional considerations, such as operating in a sunlit room, would require further mitigation to reduce background contamination of the signal for best performance.

Given the above information about spectral contribution, the ideal surgical room lighting would be white-light LEDs. The PerkinElmer Solaris system performs background correction by pulsing the excitation sources to sequentially image fluorescence emission and background light leakage to make on-line corrections. It has been shown that systems that perform some kind of background correction tend to perform better than those without;⁵⁴ this improvement in performance can also be seen from the sensitivity and linearity tests data in Sec. 4.3.

4.3 High Sensitivity to Fluorophore of Interest and Ability to Quantify In Situ

The concentrations of fluorescent agents in tissue vary by orders of magnitude depending on their distribution and targeting to specific disease biomarkers. Nonspecific agents, such as ICG, are usually administered intravenously and generally remain in the tissue at concentrations in the low micromolar range. Target-specific agents, on the other hand, are generally given time to clear normal tissue, thus will usually be present in midlow nanomolar concentrations in tissue. This poses a challenge when devices designed for ICG imaging are used to image targeted probes, as the sensitivity limits are not always optimized for low-concentration probes. All available systems were evaluated for their ability to detect and quantify signals from IRDye 800CW (LI-COR Biosciences, Lincoln, NE) in phosphate-buffered saline, through the logarithmic concentration range from 3 pM to 25 μ M. The samples were imaged individually to allow the user to modify any available gain and exposure settings and maximize the ability to detect fluorescence emission. We grouped the systems into FDA-approved imagers [Fig. 4(a)] and preclinical imagers [Fig. 4(b)]. Plots showing “ \log_{10} (fluorophore concentration)” versus “ \log_{10} (normalized fluorescence signal)” are shown in Fig. 4.

A handful of imagers also performed imaging in the 700-nm channel, so IRDye 680RD samples were used to evaluate them. As a reference, the performance was compared to the LI-COR Pearl Impulse preclinical imager, which provides over 20-bits of dynamic range, and performs imaging in an ambient-light-free chamber. Slopes of linear fits to the log-log data (slope = 1 for linearity on these log-log plots) and the lowest detectable concentrations are shown in the table of Fig. 4(d).

All imagers, under ideal conditions and dimmed lighting were able to detect down to a surface concentration of ~ 10 nM for both IRDye 800CW and IRDye 680RD (for dual-channel systems that have this channel). Thus, per this criterion, all systems seem suitable for imaging high concentrations of ICG, as intended. For imaging lower concentrations of fluorophores, it is observed that systems with higher bit depths, variable electronic gain settings, and/or background-light correction during acquisition had the best sensitivity. The VisionSense Iridium system outperforms all other instruments in terms of sensitivity to low concentrations owing to its high camera bit depth and gain adjustment (1 to 200 \times) capability. The Solaris was a close second in terms of sensitivity, again due to the high bit depth and background correction functionality based on pulsing excitation light; but the lack of gain adjustment likely limits its sensitivity below ~ 1 nM. The Fluobeam800 system with the ability to manually vary exposure time could achieve sensitivity down to ~ 5 nM, but this comes at the expense of long-exposure times on the order of seconds, which may not be feasible within a clinical setting. Similar sensitivity is obtained with the Novadaq SPY system in real-time video mode. The Quest Spectrum though equipped with a 14-bit camera compresses the image data to 8-bits at the camera output resulting in reduced sensitivity and dynamic range, which severely affected the overall system performance. In terms of quantitative ability, the closer a log-log fitted-slope (Fit equation: $\log_{10} y = m \cdot \log_{10} x + C$ which is equivalent to $y = 10^C \cdot x^m$, where m is the slope) was to 1, the more reliable a system could be for linear reporting of concentration, which was seen well with the Solaris system, owing to background correction. The Quest spectrum and VisionSense Iridium devices utilize 14-bit and 12-bit cameras, respectively, but ultimately map their data to 8-bit thus resulting in nonlinear compression and an observed slope of <1 . While VisionSense uses smart image processing algorithms to produce a wide dynamic range, the Quest Spectrum lacked such features, thus the range of detection suffers, and sensitivity is about ~ 10 nM. It should be noted that for data from VisionSense and Fluobeam fluorescence signal measurements were scaled by the gain settings and exposure times, respectively. Aside from fluorescence intensity, some systems, e.g., Novadaq SPY, may also provide perfusion and flow rate as quantitative endpoints; these measurements are usually made in software based on the fluorescence intensity data, and would hence be affected by the linearity and quantitative performance of the system as described herein. Curadel's Lab-Flare R1 was excluded from Fig. 4 as a final commercial system was unavailable for testing at the time of publishing this paper, although based upon the design the sensitivity, it was expected to be comparable to the other advanced systems and reported to be in the single nM range or better. The SurgVision system was also excluded from Fig. 4 as the sensitivity tests on this system were not available in the same methodology as used for all the other systems. However,

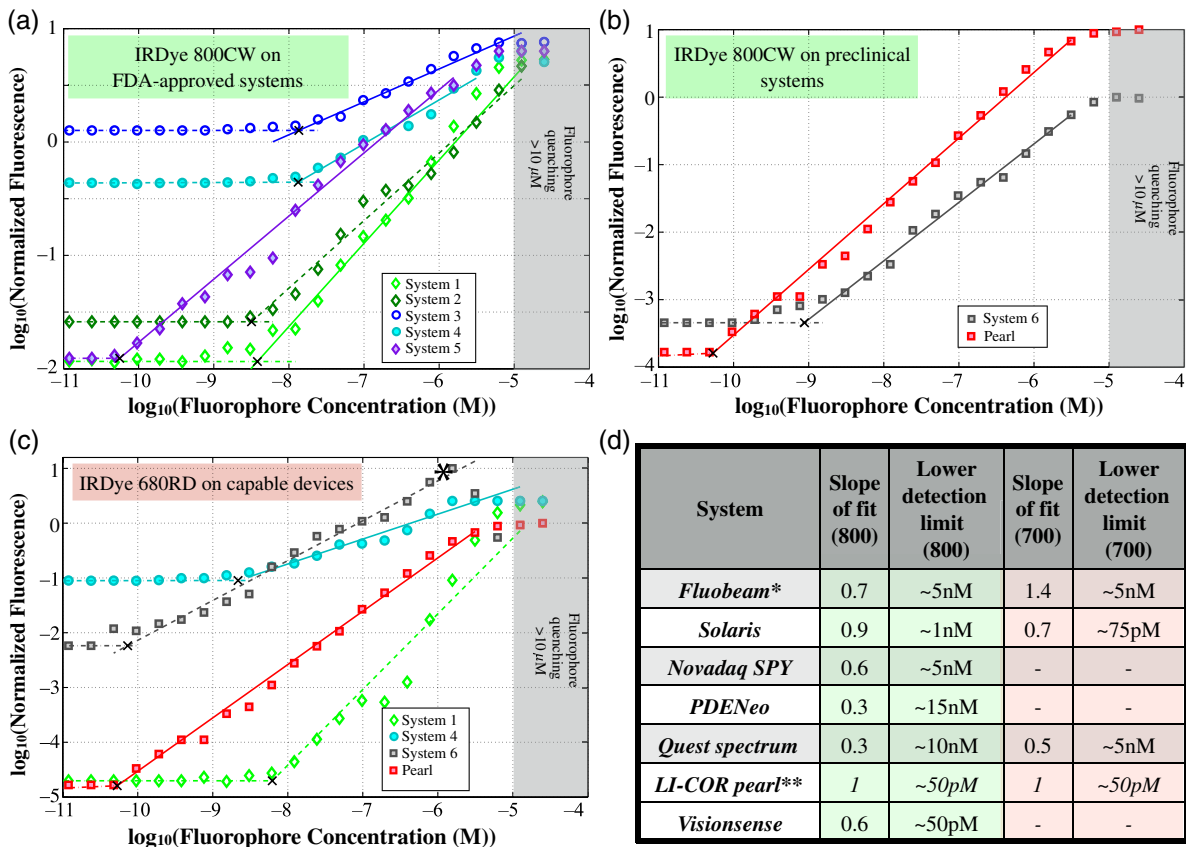


Fig. 4 Plots of \log_{10} (Fluorophore Concentration) versus \log_{10} (Normalized Fluorescence) are shown for measurements of IRDye 800CW using FDA-approved imagers (a). Panel (b) shows IRDye 800CW measurements on imagers that are not approved for clinical use. Measurements from the LI-COR pearl impulse preclinical imager are shown for comparison. Note that large variability exists in dynamic range and detection sensitivity among FDA-approved imagers. Panel (c) shows similar plots for all systems with far-red emission imaging capability when IRDye 680RD samples were tested. A handful of imagers also performed imaging in the 700-nm channel, so IRDye 680RD was tested on these. In (d), the fitted slopes and the lower limit of detection are shown. *Fluoptics has two distinct imagers, Fluobeam700 and Fluobeam800, for imaging in the 700-nm and 800-nm emission bands, respectively. **The Li-COR Pearl imager was included simply as a standard of linearity and sensitivity achievable using an enclosed light-tight imager.

the sensitivity to IRDye 800CW reported by the company is ~60 pM, which would make it among the most sensitive of the systems evaluated. This is most likely attributable to their use of an EMCCD capable of single-photon detection.

4.4 Ability to Image Multiple Fluorophores Simultaneously

Barring excitation sources and emission filters, a large part of the optics and instrumentation of an imager is more or less independent of the fluorophore being imaged within the tolerance limits on the optics. Some systems have been designed to house excitation sources for multiple excitation wavelength bands along with emission filter sets, to allow for multifluorophore imaging, either simultaneously or by switching between channels using a filter wheel. This multichannel functionality certainly adds to the cost of the device, but such a system can be a worthy investment for a research group working with multiple imaging agents, and combinations of targeted and untargeted tracers for quantification of disease biomarkers.⁴⁸ A total of three out of the eight imagers we compared are capable of multiple fluorophore imaging; the Curadel Lab-Flare R1 and the Quest Spectrum can image in the ~700- and ~800-nm channels simultaneously,

while the Solaris is capable of imaging ~470-, ~660-, ~750-, and ~800-nm channels independently (nonsimultaneous). Figure 2(d) shows an example of simultaneous white-light, 700-, and 800-nm fluorescence imaging with the merged display available on the Flare imagers.

4.5 Maximized Ergonomic Use

As a general principle, compact, portable units are easier to deploy in a surgical suite than large roll-in systems. However, the computer, display monitors, and illumination unit contribute significantly to the size and usability of a system. Studies have shown that choice of display, their location, and setup can significantly affect surgical tasks and their outcomes.⁵⁶ Currently, fluorescence-imaging systems are either compact, handheld systems such as VisionSense Iridium, Fluobeam, and PDE Neo, or larger, overhead, wheel-based systems with significant footprints such as the Solaris and Curadel systems. The former do provide mounting arms and carts to users who need them while the latter can be large enough to need a 36- to 100-ft² room for storage. Stability of images and impact of vibrations vary among devices, with larger heavier devices built for greater stability as compared to handheld systems with optional mounting

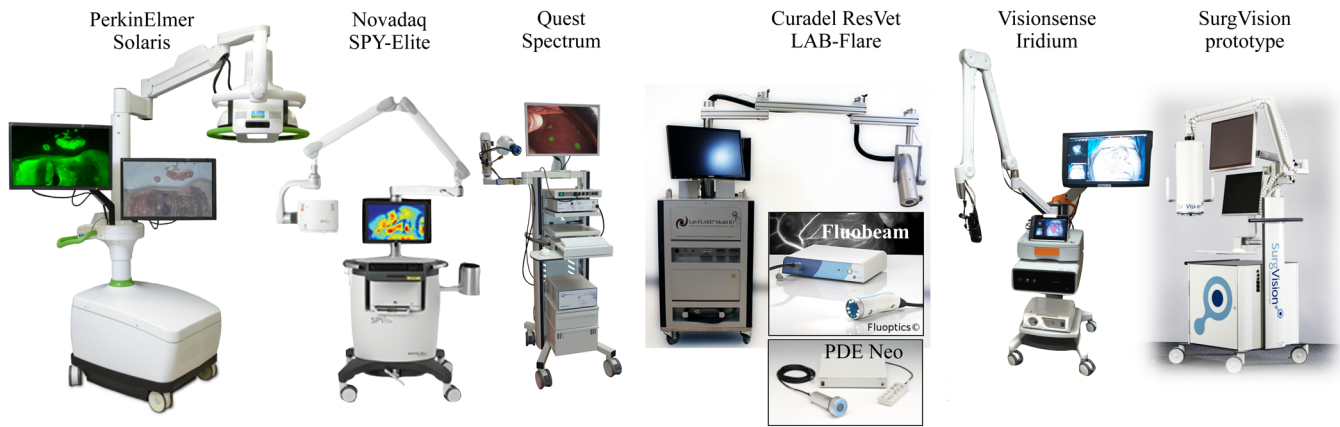


Fig. 5 Images of the leading fluorescence guidance systems evaluated here, targeted for open surgery use, shown with relative approximate size comparison. The PerkinElmer Solaris, Curadel ResVet Lab-Flare, and SurgVision Explorer Air are not 510(k) cleared for human use, while the others are for ICG procedures. All have capability to image ICG in surgical trials, with differing levels of sensitivity and features. Images from left to right are from Solaris™ Open-Air Fluorescence Imaging System, Printed with permission, (c)2015-2016 PerkinElmer, Inc., all rights reserved; NOVADAQ Spy-Elite™, copyright 2016 Novadaq Technologies Inc.; Quest Spectrum™, copyright Quest Medical Imaging; Fluobeam(R), copyright 2016 Fluoptics; Hamamatsu PDE-Neo™; Lab-FLARE(R) Model R1 copyright CURADEL; Visionsense Iridium™, copyright Visionsense; SurgVision Explorer Air prototype, image courtesy of SurgVision. All images have been printed with permission from copyright holders.

hardware. Figure 5 shows photographs of the various commercial systems. Though not to exact scale, the systems can be compared for size and physical footprint.

Handheld systems can provide better access to complex tissue geometries, such as around the head and neck or inside limbs, and are also highly mobile, whereas the larger systems generally have a wide range of functionalities such as multiple fluorophore capability, large FOV size, and large working distance. Both the PerkinElmer Solaris and Curadel Lab-Flare system have a large range of FOV sizes over which focus errors are minimal; the Lab-Flare in particular has been optimized to maintain parfocality from $0.9 \times 0.9 \text{ cm}^2$ to $25 \times 25 \text{ cm}^2$ over working distances from 12 to 18 in., enabling its usage in a wide range of surgical applications. The appropriate working distance depends directly on the intended usage, but it is interesting to note that the Solaris is the only system with a fixed working distance of 75 cm, which keeps the imaging head well out of the way of a surgeon's workspace. Along with the use of multiple excitation angles, this system attempts to provide a highly ergonomic solution to imaging fluorophores during surgery, replacing the surgical light as well. Nevertheless, as surgical applications are highly varied, ranging from inside the abdominal cavity to under the armpit, there is no single optimal design, and selecting a system will require careful consideration of its intended use. With large FOV options available on some systems, the image uniformity and quality across the field can be an important factor to consider. Qualitatively, these aspects were not significantly different across the large roll-in systems, but the handheld devices designed with lightweight optics were of acceptable but slightly poorer performance. This may or may not be significant depending on the intended clinical application, but could be important especially when fluorescence guidance is being used to save or resect fine structures, such as nerves, demanding high resolution and quality across the entire FOV.

5 Discussion

The very limited set of approved fluorophores and approved procedures, and the lack of medical reimbursement codes in

the United States for fluorescence-guided surgery procedures have kept the market for imagers in clinical imagers modest; however, owing to the direct surgical impact of these systems on surgical workflow, their overall demand continues to grow. Due to the simplicity of design, most systems are specified for operation only in the NIR-range to capture ICG emission in vessel flow, since this use remains the only approved NIR fluorescence procedure. Table 2 presents all commercially available open surgery fluorescence imagers compared on the basis of the "key desirable features" described in Sec. 4. A listing of technical specifications is also provided in Table 3. In reviewing the systems presented here, we found that the Solaris is the only openly marketed system with specifications well laid out, with the capacity to image a wide range of fluorescence emission channels. While other instruments predominantly target the ICG market, they cost about half of that of the Solaris and will be important devices for imaging the other $\sim 800\text{-nm}$ agents that are in various stages of preclinical and investigational new drug development. Meanwhile, off-label use of approved fluorophores has become increasingly common in sentinel lymph node mapping,⁵⁷ tumor resection surgeries,⁵⁸ and perfusion assessment, while identification of disease *in situ* demands the use of target-specific fluorophores.⁵⁹ This is especially true in oncological applications such as margin assessment and metastasis detection.

The development of new agents is driving technological advances by increasing the demand for new systems with lower sensitivity, shifted wavelengths, and more ergonomic set of display and usage features. The adoption of fluorescence guidance for surgery within research settings is well underway, and several imaging instrument companies have identified them as their initial target customers. This has led to emergence of several systems such as Curadel ResVet Lab-Flare and PerkinElmer Solaris that are not immediately seeking FDA approvals, but rather targeting veterinary markets at the current time. However, these systems present feature-rich capabilities with significant benefits for imaging newer test agents. As such, there is a small commercial market developing in some areas for these research units, which will pave the way for future

Table 2 Comparison of the various commercial fluorescence imagers for open-surgical applications based on the key operational factors.

Feature	PerkinElmer Solaris	Fluoptics Fluobeam 800	Curadel Lab-Flare	Quest Spectrum	Novadaq SPY Elite	Hamamatsu PDE Neo	VisionSense Iridium	SurgVision Explorer Air
<i>Real-time white-light and fluorescence overlay</i>	Yes	No	Yes	Yes	No	No	Yes	Yes
<i>Room lights</i>	On	Low	Low	On	Low	Low	Low	On
<i>Background correction</i>	Yes	No	No	Yes	No	No	No	Yes
<i>Sensitivity</i>	~1nM	~5nM	NA	~10nM	~5nM	~15nM	~50pM ^a	~60pM ^d
	~75pM	—	NA	~5nM	—	—	—	—
<i>Quantification—Linearity</i>	★★★★	★★★★	NA	★	★★★★	★	★★★★	★★★★
<i>Multifluorophore imaging</i>	4	1	2	2	1	1	1	1
<i>Channels</i>	No	—	Yes	Yes	—	—	—	—
<i>Simultaneous</i>	★★★★	★★★★	★★★★	★★★★	★★	★	★★★★	NA
<i>Ergonomics</i>	Yes	Yes	Yes	No ^b	Yes	No	No	Yes
<i>Raw data export</i>	~75	15 to 25	30 to 45	~30	~30	~30	~30	15 to 50
<i>Working distance (cm)</i>	Yes	Yes	Yes	No	No	Yes	No	No
<i>Variable FOV</i>	2+	1+	2+	1	2	1	1	2
<i>Number of display monitors</i>	Overhead-fixed	Arm+Handheld	Overhead-mobile	Arm+Handheld	Overhead-mobile	Arm+Handheld	Arm+Handheld	Overhead-mobile
<i>Mount type</i>	•••••	•	•••••	•••	•••	•	••	•••
<i>Size</i>	No	Yes	No	Yes	Yes	Yes	Yes	No
<i>FDA approved</i>	\$\$\$\$\$	\$\$	\$\$\$\$	\$\$	\$\$	\$	\$\$	\$\$\$\$
<i>Cost^f</i>	Sensitive to low concentrations, four fluorescence channels	Compact, good sensitivity	Excellent optics, large range of FOV	Simultaneous white-light, multichannel fluorescence overlay	Trade-off between cost and functionality	Compact, low cost	Sensitive to low concentrations, and overlay capability	Sensitivity to low concentrations
<i>Best strength</i>	Not set up for expansion to simultaneous multichannel imaging	No white-light imaging	Commercial system unavailable at the time of testing	Nonlinear	No white-light overlay	No white-light imaging, nonlinear	Single fluorescence channel	Single fluorescence channel on the commercial system
<i>Weakness</i>	^a VisionSense Iridium has an FDA-approved unit with 805-nm excitation laser. For the sensitivity test, a 785-nm laser was used, which VisionSense sells as a research-only option. ^b Quest offers a research-only custom-designed option on the Spectrum system that has 12-bit raw data export capability, such a system designed to our specifications was unavailable at the time of writing this article, and all tests were performed using the FDA-approved version of the system. ^c Total cost is inclusive of only the device initial cost, so that any yearly maintenance costs, license costs, and cost of disposables, if any, were not factored in. However, annual recurring service fee costs are conventionally 10% to 20% of the initial cost, and prices of disposables can vary widely between systems. ^d Sensitivity test data from the SurgVision prototype system were performed not performed using the same methodology as others NA = information not available.							

Table 3 Technical specifications for each system analyzed are shown, broken down into the illumination features, emission filter features, camera specifications, optical design, and image output features.

Company	PerkinElmer	Fluoptics	Curadel	Quest	Novadaq	Hamamatsu	VisionSense	SurgVision
Device	Solaris	Fluobeam 800(700)	LAB-Flare	Spectrum ^a	SPY Elite	PDE	Iridium ^b	Explorer Air
Optical irradiance	NS	5 mW/cm ²	NS	NS	4-31 mW/cm ²	4.0 mW/cm ²	NS	NS
Excitation light source	Filtered LEDs (488SP, 667SP, 743SP, 757SP)	750 (680)-nm Laser	665 ± 3 nm; 760 ± 3 nm	LEDs	805-nm laser	760-nm LEDs	805-nm Laser	760-nm LEDs
Emission filters	516 to 523 nm, 692 to 742 nm, 770 to 809 nm, 784LP	>800 (700)-nm Longpass	685 to 735 nm and >781 nm	700 to 830; 830 to 1000 nm	825 to 850 nm	NS	825 to 850 nm	NS
Filter OD	6	NS	NS	NS	NS	NS	NS	NS
Fluorescence camera	Zyla 5.5	NS	NS	NS	NS	NS	NS	NS
Sensor type	sCMOS	CCD	CCD	CCD	CCD	CCD	CCD	EMCCD
Read-out bits	16	8	10	12	8	8	12	NS
Exposure time	1 ms	1 ms to 1 s	66 μs to 3 s	NS	NS	NS	NS	NS
Full well depth	30,000 e ⁻	NS	NS	NS	NS	NS	NS	180,000 e ⁻
Maximum frame rate (fps)	100	25	30	20	NS	NS	NS	56
Variable gain setting	No	No	Yes	NS	No	No	Yes	NS
Optics	~75	15 to 25	30 to 45	~30	~30	~30	~30	15 to 50
Working distance (cm)	2	2 to 3	NS	NS	NS	NS	NS	NS
Depth of field (cm)	10 × 10 to 2.5 × 2.5	2.2 × 1.5 to 20 × 14	0.9 × 0.9 to 25.3 × 25.3	NS	19 × 14	5 × 5 to 10 × 6.7	19 × 14	15 × 15
FOV (cm ²)								
Image output	1024 × 1024	720 × 576	1024 × 1024	NS	1024 × 768	640 × 480	960 × 720	512 × 512
Pixel dimensions	100 μm	300 to 50 μm	500 to 50 μm	NS	NS	NS	NS	NS
Resolution	12	8	10	8	8	8	8	8
Bit depth (bit)								

^aQuest Spectrum specifications are for the FDA-approved system. Quest offers customization options on the excitation sources, emission filter sets, and 12-bit data export capability on their custom research units.

^bVisionSense specifications are for the FDA-approved system. They offer a custom 785 nm excitation laser option, with matching emission filter set for research users. Note: NS = not specified.

indications and potential FDA clearance applications. There are also companies such as Quest Medical Imaging, Curadel, and SurgVision that are designing high-end systems customizable to the specific requirements of their research users through industry-academic partnerships. The number of these non-cleared systems will likely grow as the field of fluorescence-guided surgical research develops.

In this study, ICG was not used for testing, since this molecule is well known to be of low fluorescence yield and unsuitable for specific binding to other proteins. The IRDye candidates used here are only one set of possible agents, but specifically IRDye 800CW is one that has been used in several human clinical trials, and was specifically designed and supported for protein binding, while preserving the high molar absorption coefficient and emission quantum yield. So while the testing was completed for IRDyes 800CW and 680RD, other candidate agents will have shifted spectra as well, and sensitivity testing should be carried out as needed to validate the lower level of sensitivity, as shown in the results here of Fig. 4. As mentioned above though, the linearity results here are likely universal, while a shift in the spectrum of the dye would typically affect only the lower-level sensitivity limit.

In the near-term, it should be expected that several new systems will be launched in the coming months, including the SurgVision imager, which is similar in optical-filtering design to the Lab-Flare instrument but uses a single EMCCD-based fluorescence camera and customizable emission filters. All commercial multispectral fluorescence imagers are still in a preclinical development phase and the exact FDA clearance trajectory for these systems is not yet clear. This new trend in development of customizable systems built to user specifications with flexibility in choice of excitation and emission wavelengths will likely have its own trajectory, with leading research users seeking local institutional review board approvals for research use, allowing the use of more fully featured systems in a trial, rather than waiting for an FDA-cleared versions with fixed specifications. This will certainly impact the drug discovery and development processes. In the long term, it should be expected that a fair amount of reorganization and consolidation could occur, as the industry converges on what the eventual demands will be from a clinical point of view, and based on what is needed for further research and development. To date, with the exception of PerkinElmer, the larger imaging companies have remained on the sideline in the open surgery area. Notable exceptions are the advances of Olympus, Leica, and Zeiss in other surgical specialties such as endoscopy and neurosurgery. However, the specialized systems will likely reach a level of success first through 510(k) clearance for conventional ICG imaging and likely be used off-label for clinical research in agents for open surgery. This process is happening now, and these more feature-rich systems will lead to an industry specialization around the indications that have the most clinical adopters and most promising trials.

6 Conclusions

In summary, a proposed set of “desirable features” has been described, in descending order of importance; these are suggested to be the right judgment criteria for evaluating a fluorescence-imaging device for open-surgical use. These criteria and the results of the analysis are based on extensive testing and evaluation of each FDA-approved and preclinical imager presented here. *Real-time fluorescence overlay on RGB white-light images and fluorescence-mode operation under ambient*

room lighting are proposed as the most important requirements because these aspects limit the utility of a system if not present, irrespective of its sensitivity. *Sensitivity to low fluorophore concentrations* and the *ability to linearly quantify relative fluorophore concentrations* are next most important in rank order, as these will ultimately determine the clinical use of the imaging device. Furthermore, as the adoption of fluorescence imaging to guide surgery continues to grow, the quantitative ability will play an important role in comparing data from multicenter trials, and comparing results spatially and longitudinally both within and among patients. Next, *simultaneous multifluorophore imaging capability* is an “extra” feature to most users but can be critical for research laboratories developing next-generation imaging agents and methods to improve cancer extent and margin assessment using combinations of imaging agents. Lastly, we discussed *ergonomics* as the final important criterion for selecting a system, as this is again greatly tied to system utility during surgery. While we have proposed this set of desirable features, each system does come with its own set of positive and negative aspects and there is no single “best” system in the market. The intention of this review paper is to help simplify the task of selecting the right system to invest in for both translational clinical trials and preclinical or veterinary research

Acknowledgments

This work was funded by the National Institutes of Health research under Grant No. R01CA109558. We would like to thank Jason R. Gunn at Thayer School of Engineering, Hanover NH, for his help in communicating with companies and the preparation of test samples. We appreciate the help from Quest Medical Imaging, Visionsense, PerkinElmer, Curadel ResVet Imaging, Fluoptics, NOVADAQ, Mitaka USA (distributors for Hamamatsu PDE) for allowing demos of the devices, imaging the samples provided by us, voluntarily sharing the acquired image data with us, and providing photographs of their imaging devices for reprint in this article. We thank SurgVision for sharing imaging data, and photographs of their prototype imager.

References

1. E. L. Rosenthal et al., “Successful translation of fluorescence navigation during oncologic surgery: a consensus report,” *J. Nucl. Med.* **57**(1), 144–150 (2016).
2. S. Gioux, H. S. Choi, and J. V. Frangioni, “Image-guided surgery using invisible near-infrared light: fundamentals of clinical translation,” *Mol. Imaging* **9**(5), 237–255 (2010).
3. B. Zhu and E. M. Sevick-Muraca, “A review of performance of near-infrared fluorescence imaging devices used in clinical studies,” *Br. J. Radiol.* **88**(1045), 20140547 (2015).
4. Q. T. Nguyen and R. Y. Tsien, “Fluorescence-guided surgery with live molecular navigation—a new cutting edge,” *Nat. Rev. Cancer* **13**(9), 653–662 (2013).
5. R. K. Orosco, R. Y. Tsien, and Q. T. Nguyen, “Fluorescence imaging in surgery,” *IEEE Rev. Biomed. Eng.* **6**, 178–187 (2013).
6. S. B. Mondal et al., “Real-time fluorescence image-guided oncologic surgery,” *Adv. Cancer Res.* **124**, 171–211 (2014).
7. C. Chi et al., “Intraoperative imaging-guided cancer surgery: from current fluorescence molecular imaging methods to future multi-modality imaging technology,” *Theranostics* **4**(11), 1072–1084 (2014).
8. J. T. Alander et al., “A review of indocyanine green fluorescent imaging in surgery,” *Int. J. Biomed. Imaging* **2012**, 940585 (2012).
9. E. L. Rosenthal et al., “The status of contemporary image-guided modalities in oncologic surgery,” *Ann. Surg.* **261**(1), 46–55 (2015).
10. G. M. van Dam et al., “Intraoperative tumor-specific fluorescence imaging in ovarian cancer by folate receptor-alpha targeting: first in-human results,” *Nat. Med.* **17**(10), 1315–1319 (2011).

11. Q. T. Nguyen et al., "Surgery with molecular fluorescence imaging using activatable cell-penetrating peptides decreases residual cancer and improves survival," *Proc. Natl. Acad. Sci. U.S.A.* **107**(9), 4317–4322 (2010).
12. E. N. Savariar et al., "Real-time in vivo molecular detection of primary tumors and metastases with ratiometric activatable cell-penetrating peptides," *Cancer Res.* **73**(2), 855–864 (2013).
13. M. B. Sturm et al., "Targeted imaging of esophageal neoplasia with a fluorescently labeled peptide: first-in-human results," *Sci. Transl. Med.* **5**(184), 184ra161 (2013).
14. M. Bouvet and R. M. Hoffman, "Glowing tumors make for better detection and resection," *Sci. Transl. Med.* **3**(110), 110fs110 (2011).
15. N. J. Harlaar et al., "Real-time near infrared fluorescence (NIRF) intraoperative imaging in ovarian cancer using an $\alpha_v\beta_3$ -integrin targeted agent," *Gynecol. Oncol.* **128**(3), 590–595 (2013).
16. K. S. Samkoe et al., "Quantitative in vivo immunohistochemistry of epidermal growth factor receptor using a receptor concentration imaging approach," *Cancer Res.* **74**(24), 7465–7474 (2014).
17. G. E. Moore et al., "The clinical use of fluorescein in neurosurgery; the localization of brain tumors," *J. Neurosurg.* **5**(4), 392–398 (1948).
18. F. Acerbi et al., "Fluorescein-guided surgery for malignant gliomas: a review," *Neurosurg. Rev.* **37**(4), 547–557 (2014).
19. W. Stummer et al., "Fluorescence-guided surgery with 5-aminolevulinic acid for resection of malignant glioma: a randomised controlled multicentre phase III trial," *Lancet Oncol.* **7**(5), 392–401 (2006).
20. S. Zhao et al., "Intraoperative fluorescence-guided resection of high-grade malignant gliomas using 5-aminolevulinic acid-induced porphyrins: a systematic review and meta-analysis of prospective studies," *PLoS One* **8**(5), e63682 (2013).
21. P. A. Valdes et al., "Quantitative fluorescence using 5-aminolevulinic acid-induced protoporphyrin IX biomarker as a surgical adjunct in low-grade glioma surgery," *J. Neurosurg.* **123**(3), 771–780 (2015).
22. M. Rink et al., "Hexyl aminolevulinic acid-guided fluorescence cystoscopy in the diagnosis and follow-up of patients with non-muscle-invasive bladder cancer: a critical review of the current literature," *Eur. Urol.* **64**(4), 624–638 (2013).
23. S. P. Lerner and A. Goh, "Novel endoscopic diagnosis for bladder cancer," *Cancer* **121**(2), 169–178 (2015).
24. D. Jocham et al., "Improved detection and treatment of bladder cancer using hexaminolevulinic acid imaging: a prospective, phase III multicenter study," *J. Urol.* **174**(3), 862–866 (2005).
25. M. C. Loning et al., "Fluorescence staining of human ovarian cancer tissue following application of 5-aminolevulinic acid: fluorescence microscopy studies," *Lasers Surg. Med.* **38**(5), 549–554 (2006).
26. R. Vanseviciute et al., "5-aminolevulinic-acid-based fluorescence spectroscopy and conventional colposcopy for in vivo detection of cervical pre-malignancy," *BMC Women's Health* **15**, 35 (2015).
27. S. Andrejevic-Blant et al., "Time-dependent hexaminolevulinic acid induced protoporphyrin IX distribution after topical application in patients with cervical intraepithelial neoplasia: a fluorescence microscopy study," *Lasers Surg. Med.* **35**(4), 276–283 (2004).
28. A. M. Smith, M. C. Mancini, and S. Nie, "Bioimaging: second window for in vivo imaging," *Nat. Nanotechnol.* **4**(11), 710–711 (2009).
29. A. Matsui et al., "Real-time intra-operative near-infrared fluorescence identification of the extrahepatic bile ducts using clinically available contrast agents," *Surgery* **148**(1), 87–95 (2010).
30. M. Sekijima et al., "An intraoperative fluorescent imaging system in organ transplantation," *Transplant. Proc.* **36**(7), 2188–2190 (2004).
31. J. Watanabe et al., "Evaluation of the intestinal blood flow near the rectosigmoid junction using the indocyanine green fluorescence method in a colorectal cancer surgery," *Int. J. Colorectal Dis.* **30**(3), 329–335 (2015).
32. S. F. Chen et al., "The application of intraoperative near-infrared indocyanine green videoangiography and analysis of fluorescence intensity in cerebrovascular surgery," *Surg. Neurol. Int.* **2**, 42 (2011).
33. J. Caesar et al., "The use of indocyanine green in the measurement of hepatic blood flow and as a test of hepatic function," *Clin. Sci.* **21**, 43–57 (1961).
34. A. Raabe et al., "Near-infrared indocyanine green video angiography: a new method for intraoperative assessment of vascular flow," *Neurosurgery* **52**(1), 132–139 (2003).
35. C. Holm et al., "Intraoperative evaluation of skin-flap viability using laser-induced fluorescence of indocyanine green," *Br. J. Plast. Surg.* **55**(8), 635–644 (2002).
36. B. T. Lee et al., "The FLARE™ intraoperative near-infrared fluorescence imaging system: a first-in-human clinical trial in perforator flap breast reconstruction," *Plast. Reconstr. Surg.* **126**(5), 1472–1481 (2010).
37. N. D. Desai et al., "A randomized comparison of intraoperative indocyanine green angiography and transit-time flow measurement to detect technical errors in coronary bypass grafts," *J. Thorac. Cardiovasc. Surg.* **132**(3), 585–594 (2006).
38. D. P. Taggart et al., "Preliminary experience with a novel intraoperative fluorescence imaging technique to evaluate the patency of bypass grafts in total arterial revascularization," *Ann. Thorac. Surg.* **75**(3), 870–873 (2003).
39. M. V. Marshall et al., "Near-infrared fluorescence imaging in humans with indocyanine green: a review and update," *Open Surg. Oncol. J.* **2**(2), 12–25 (2010).
40. T. Kitai et al., "Fluorescence navigation with indocyanine green for detecting sentinel lymph nodes in breast cancer," *Breast Cancer* **12**(3), 211–215 (2005).
41. S. L. Troyan et al., "The FLARE intraoperative near-infrared fluorescence imaging system: a first-in-human clinical trial in breast cancer sentinel lymph node mapping," *Ann. Surg. Oncol.* **16**(10), 2943–2952 (2009).
42. A. L. Vahrmeijer et al., "Image-guided cancer surgery using near-infrared fluorescence," *Nat. Rev. Clin. Oncol.* **10**(9), 507–518 (2013).
43. B. W. Pogue et al., "Vision 20/20: molecular-guided surgical oncology based upon tumor metabolism or immunologic phenotype: technological pathways for point of care imaging and intervention," *Med. Phys.* **43**(6), 3143–3156 (2016).
44. H. S. Choi et al., "Targeted zwitterionic near-infrared fluorophores for improved optical imaging," *Nat. Biotechnol.* **31**(2), 148–153 (2013).
45. B. Zhu, J. C. Rasmussen, and E. M. Sevick-Muraca, "A matter of collection and detection for intraoperative and noninvasive near-infrared fluorescence molecular imaging: to see or not to see?" *Med. Phys.* **41**(2), 022105 (2014).
46. M. A. Whitney et al., "Fluorescent peptides highlight peripheral nerves during surgery in mice," *Nat. Biotechnol.* **29**(4), 352–356 (2011).
47. A. Matsui et al., "Real-time, near-infrared, fluorescence-guided identification of the ureters using methylene blue," *Surgery* **148**(1), 78–86 (2010).
48. K. M. Tichauer et al., "Microscopic lymph node tumor burden quantified by macroscopic dual-tracer molecular imaging," *Nat. Med.* **20**(11), 1348–1353 (2014).
49. J. T. Liu et al., "Quantifying cell-surface biomarker expression in thick tissues with ratiometric three-dimensional microscopy," *Biophys. J.* **96**(6), 2405–2414 (2009).
50. A. V. DSouza et al., "Logarithmic intensity compression in fluorescence guided surgery applications," *J. Biomed. Opt.* **20**(8), 080504 (2015).
51. Z. Chen, X. Wang, and R. Liang, "RGB-NIR multispectral camera," *Opt. Express* **22**(5), 4985–4994 (2014).
52. T. Handa et al., "New device for intraoperative graft assessment: HyperEye charge-coupled device camera system," *Gen. Thorac. Cardiovasc. Surg.* **58**(2), 68–77 (2010).
53. J. T. Elliott et al., "Review of fluorescence guided surgery visualization and overlay techniques," *Biomed. Opt. Express* **6**(10), 3765–3782 (2015).
54. K. Sexton et al., "Pulsed-light imaging for fluorescence guided surgery under normal room lighting," *Opt. Lett.* **38**(17), 3249–3252 (2013).
55. B. Zhu, J. C. Rasmussen, and E. M. Sevick-Muraca, "Non-invasive fluorescence imaging under ambient light conditions using a modulated ICCD and laser diode," *Biomed. Opt. Express* **5**(2), 562–572 (2014).
56. G. B. Hanna, S. M. Shimi, and A. Cuschieri, "Task performance in endoscopic surgery is influenced by location of the image display," *Ann. Surg.* **227**(4), 481–484 (1998).
57. M. Plante et al., "Sentinel node mapping with indocyanine green and endoscopic near-infrared fluorescence imaging in endometrial cancer. A pilot study and review of the literature," *Gynecol. Oncol.* **137**(3), 443–447 (2015).
58. H. J. Handgraaf et al., "Intraoperative fluorescence imaging to localize tumors and sentinel lymph nodes in rectal cancer," *Minim. Invasive Ther. Allied Technol.* **25**(1), 48–53 (2016).
59. M. Koch and V. Ntziachristos, "Advancing surgical vision with fluorescence imaging," *Annu. Rev. Med.* **67**, 153–164 (2016).

Alisha V. DSouza is a postdoctoral research associate at Thayer School of Engineering at Dartmouth College. She received her PhD in engineering sciences from Dartmouth, where she worked in Prof. Brian Pogue's lab in the area of fluorescence imaging and tomography for noninvasive metastasis sensing. Prior to her PhD she received her bachelor of engineering degree in electronics and communication from Manipal Institute of Technology, India.

Huiyun Lin received her PhD in optical engineering from Fujian Normal University, China in 2012. Currently, she is an associate professor at the School of Photonics and Electronic Engineering at Fujian Normal University. She was a visiting scholar at Thayer School of Engineering at Dartmouth College under Prof. Brian W. Pogue in 2015, where she was involved the study of Cherenkov excited luminescence imaging in radiation therapy. Her research interests include the time and spectrally resolved singlet oxygen luminescence measurements.

Eric R. Henderson is an assistant professor of orthopaedic surgery at Dartmouth. He completed medical school and orthopedic residency at the University of South Florida and completed an orthopedic oncology

fellowship at Massachusetts General Hospital. He practices orthopedic oncology at Dartmouth-Hitchcock Medical Center.

Kimberley S. Samkoe is an assistant research professor in the Department of Surgery at Dartmouth Medical School and holds a PhD in biophysical chemistry from the University of Calgary, Canada. She has particular interest in fluorescence imaging with applications for cancer diagnosis and therapy monitoring, including in vivo quantification of protein receptors, photodynamic therapy, and contrast-enhanced image guidance for dosimetry and therapeutic response of solid tumors.

Brian W. Pogue is professor of engineering, physics, and surgery at Dartmouth College, having a PhD from McMaster University Canada. He works on novel imaging systems for surgery and radiation therapy guidance. He has published >300 peer-reviewed and >400 conference papers, on work funded by NCI, NIBIB, and DoD. He is on editorial boards for *Physics in Medicine & Biology*, *Medical Physics*, *Journal of Biomedical Optics*, and *Breast Cancer Research* and is an elected Fellow of the OSA and AIMBE.